Damage Evolution in Physical Scale Model Tests of a Stretch of the Breakwater of Peniche Harbour

Rute Lemos, Conceição Fortes, João Alfredo Santos, and Ana Mendonça

Abstract During physical scale model tests of rubble mound breakwaters, the assessment of the eroded volume of the armour layer subjected to incident sea waves can be determined from consecutive surveys of the surface of the armour layer after each test run. This enables one to assess the damage level of the structure by comparing erosion profiles and by the eroded volume between consecutive surveys of the tested section. The present study aimed to evaluate the damage evolution of a section of the Peniche harbour west breakwater, whose armour layer is made of tetrapods, A dimensionless damage parameter was computed, based on the eroded volume at the end of each test. The test program consisted of three test series (A, B and C) with different durations and wave conditions sequences, considering the low-water level (water depth of 0.20 m at the toe of the structure) and high-water level (0.24 m) and sea states with peak periods Tp = 1.70 s and Tp = 1.98 s and significant wave heights, H_{m0}, ranging between 0.12 m and 0.19 m. The model was built and operated according to Froude's similarity law, with a geometrical scale of 1:50. The eroded volume assessment was done by means of armour layer surveys based on the Time of Flight (ToF) methodology, using a Kinect sensor position. The surveys produced 3D surface models, at the beginning and the end of the test series, when the whole extension of the armour layer was dry and visible, and after each intermediate test, when part of the armour layer was submerged. A comparative analysis was made, based upon the damage level obtained with the three different test series (with different durations and wave conditions sequences).

Keywords Breakwater · Damage evolution · Position sensor · 3D surface model

R. Lemos (✉) · C. Fortes · A. Mendonça
LNEC—Laboratório Nacional de Engenharia Civil, Lisbon, Portugal
e-mail: rlemos@lnec.pt

J. A. Santos
ISEL—Instituto Superior de Engenharia de Lisboa, Instituto Politécnico de Lisboa, Lisbon, Portugal

CENTEC—Centre for Marine Technology and Ocean Engineering, Instituto Superior Técnico, Lisbon, Portugal

C. Chastre et al. (eds.), *Testing and Experimentation in Civil Engineering*,
RILEM Bookseries 41, https://doi.org/10.1007/978-3-031-29191-3_31

1 Introduction

To optimize the hydraulic design of rubble-mound breakwaters, physical scale model tests are often necessary and overtopping and hydraulic stability tests are the most common ones.

The assessment of the damage evolution (in stability tests) during scale model tests of rubble-mound breakwaters is traditionally made by comparing the erosion profiles, which are representative of the tested section, and by determining the eroded volume of the tested section between consecutive surveys. Armour layer damage is then characterized by parameters based either on the number of displaced armour units, as is the Nod parameter [1], or on dimensionless parameters based on the eroded area of a profile of the armour layer, such as S (Broderick and Ahrens 1982) or the eroded depth, E [2, 3].

Recently, several techniques have been developed for surveying the outer envelope of the armour layer of rubble-mound breakwaters in scale model tests. A review of these techniques can be found in Campos et al. [4]. Such techniques include photogrammetry, LIDAR and Time of Flight systems, which enable very accurate 3D surface models of the armour layer of the breakwater model to be obtained. In this context, [5] and [6] used a procedure for reconstructing submerged scenes from stereo-photos where the refraction at the air-water interface is corrected, thus allowing the surveys of the armour layer surface to be made without the need to empty the flume or tank where the tests take place. More recently, Musumeci [7], Sande et al. [8] and Lemos et al. [6] used a methodology using a position sensor which enabled to gather 3D scans of armour layers composed by cubipods and Antifer cubes.

This paper describes three scale model test series (A, B and C) whose objective was to evaluate damage evolution of a stretch of the Peniche harbour west breakwater whose armour layer is made of tetrapods.

For test series A (a long-duration test series), each wave condition was run until damage stabilization occurs, beginning with the lowest water level in an increasing intensity sequence. Test series B and C were intended to simulate damage from a sequence of individual storms with a well-defined duration. Test Series B was carried out with increasing water levels whereas test series C was carried out with decreasing water levels.

After this introductory section, the experimental facilities and the tests carried out are presented in Sect. 2. Section 3 presents the procedures for surveying the armour layer, whereas in Sect. 4, the results obtained are presented and discussed. The paper ends with the conclusions chapter.

2 Physical Model and Test Conditions

The experiments were performed at the Ports and Maritime Structures Unit (NPE) of the Hydraulics and Environment Department of the Portuguese Laboratory for

Civil Engineering (LNEC), in the COI1 wave flume, which is approximately 50 m long, with an operating width of 0.8 m and an operating water depth of 0.8 m. The flume is equipped with a piston-type wave-maker that combines both irregular wave generation and dynamic absorption of reflected waves identified with two wave gauges located in front of the wave paddle (Fig. 1).

The model was built and operated according to Froude's similarity law, with a geometrical scale of 1:50. The armour layer was made of 160 kN tetrapods laid on a slope of approximately 2:3. The prototype cross-section is presented in Fig. 2.

The bottom of the wave flume has a 26 m long smooth slope (1.6%), followed by a 4.3% slope that represented the sea bottom in front of the breakwater section (Fig. 3).

Ten resistive-type wave gauges were deployed along the wave flume. The wave gauges AW1 and AW2 measured the wave conditions near the wavemaker, while probes S1 to S5 characterized the wave propagation along the flume.

The wave parameters used to describe the test conditions are those obtained close to the wave generator.

Figure 4 illustrates an overview of the cross-section built in the flume.

Fig. 1 Overview of the irregular wave flume COI1

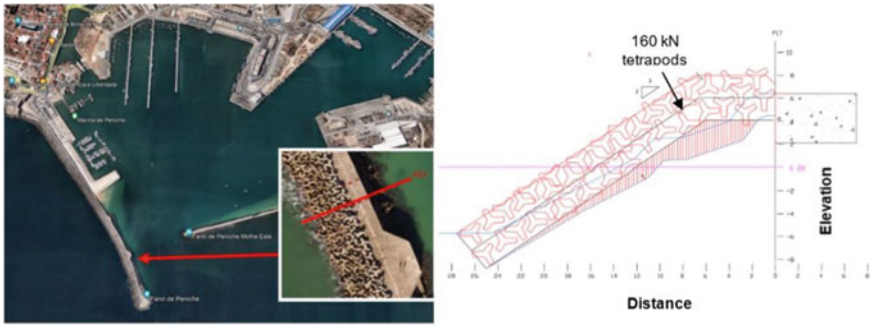

Fig. 2 Section location and characteristics

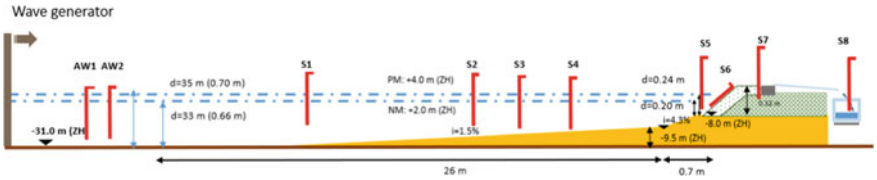

Fig. 3 Bottom and layout of the resistive wave gauges along the flume

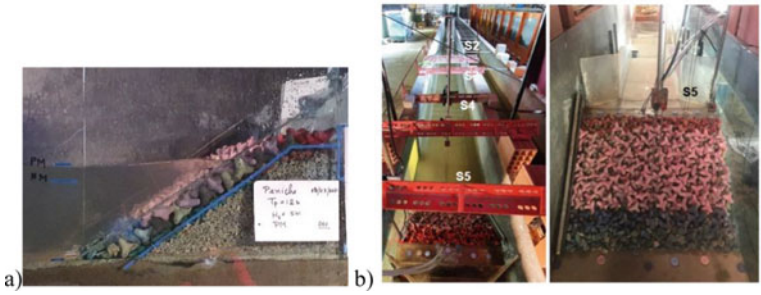

Fig. 4 Cross section of Peniche breakwater and resistive wave probes along the flume

The tests were carried out considering two sea water levels: the low-water level (LWL), with a water depth of 0.20 m at the toe of the structure and a depth of 0.66 m at the deepest part of the flume and the high-water level (HWL), with a water depth of 0.24 m at the toe of the structure and a depth of 0.70 m at the deepest part of the flume.

The wave conditions considered were peak periods of 1.70 s and 1.98 s (12 s and 14 s at prototype, respectively) and significant wave heights, of 0.12 m, 0.14 m and 0.16 m. (6.0 m, 7.0 m and 8.0 m at prototype, respectively). Table 1 summarizes the considered test conditions.

The longest test series, series A, aims to confirm the stabilization of damage of the armour layer when subjected to a sea state with constant characteristics. Thus, a given test condition, characterized by a significant wave height (H_{m0}) and peak period, (T_p) with a duration of 1000 waves, is repeated until the number of armour units displaced from their original position does not change at the end of two consecutive tests.

Then, the test series continues, using the next test condition, with increasing energy. The test sequence started with the mean water level, and then it changed to the high-water level.

Test series B and C have limited test durations. Test B was conducted with increasing water levels and peak periods and test C with decreasing water levels and peak periods.

Each test series was carried out without reconstruction of the model.

Table 1 Water levels and wave conditions for test series A, B and C

Series	Test	T_p (s)	Hm0 (m)	Depth at the toe (m)	Test duration (s)	Number of test runs	Test runs
A	1	1.70	0.12	0.13	1680	Until damage stabilization	T59–T61
	2	1.70	0.14	0.13	1680		T62–T65
	3	1.70	0.16	0.13	1680		T66–T69
	4	1.98	0.14	0.17	1980		T70–T73
	5	1.98	0.16	0.17	1980		T74–T77
	6	1.98	0.18	0.17	1980		T78–T81
B	1	1.70	0.12	0.13	1680	1	T82
	2	1.70	0.14	0.13	1680	4	T83–T86
	3	1.70	0.16	0.13	1680	4	T87–T90
	5	1.98	0.18	0.17	1980	4	T91–T94
	6	1.98	0.16	0.17	1980	4	T95–T98
C	4	1.98	0.14	0.17	1980	2	T99 and T100
	5	1.98	0.16	0.17	1980	4	T101–T104
	6	1.98	0.18	0.17	1980	4	T105–T108
	2	1.70	0.14	0.13	1680	4	T109–T112
	3	1.70	0.16	0.13	1680	4	T113–T116

3 Materials and Methods

The definition of damage in rubble mound breakwaters depends on aspects such as the typology, design, armour unit type, or the functional requirements of the structure. Damage is usually defined by the degree of reshaping of the armour layer and therefore associated to the failure mode and can be quantified by the eroded volume or number of units removed [9].

Damage characterization can be achieved by using an adequate damage descriptor, as the commonly used displacement counting method, where damage, D, can be related to any definition of movements including rocking. The relative number of moving units can also be related to the total number of units inside a vertical strip of width D_n (the nominal diameter) stretching from the bottom to the top of the armour layer. For this strip displacement definition [1] used the term Nod for units displaced out of the armour layer and Nor for rocking units. The disadvantage of Nod and Nor is the dependence of the slope (strip) length [10].

Table 2 Thresholds of S for different damage levels, for non-overtopped two-layers conventional breakwaters, according to [12] and the Rock Manual (2007) (adapted from Campos et al. [4, 9])

	Dimensionless eroded parameter (S)						
	Threshold 1		Threshold 2–3			Threshold 4	
Cot α	Damage initiation	Start of damage	Iribarren's damage	Initiation of destruction	Intermediate damage	Destruction	Failure
1.5	1.5	2	2.5	6.5	3–5	12	8
2	2	2	3	8	4–6	14	8
3	2.5	2	3.5	9.5	6–9	16	12
4	3	3	4	11	8–12	18	17

The damage descriptor used in the present work was the dimensionless damage parameter $S = \frac{A_e}{D_n^2} S = \frac{A_e}{D_n^2} S = \frac{A_e}{D_n^2}$, defined by Broderick [11] where A_e is the eroded area of the profile and D_n is the nominal diameter of the block. S can be interpreted as the number of squares with side length D_{n50} which fit into the eroded area.

The improvements and availability of accurate 3D survey techniques based on scanning instruments as LIDAR and photogrammetry techniques, as well as the development of artificial vision algorithms make it possible to combine different damage descriptors.

This was the case of the present study. As the damage parameter S is less suitable in the case of complex types of armour units like tetrapods, due to the difficulty in defining a surface profile, to minimize this uncertainty it was decided to compute the mean eroded area by using the total eroded volume of the entire armour layer.

By dividing the eroded volume (Ev) at the end of a test run by the section usable width (X, in this case 0.72 m), one obtained the section mean eroded area ($A_e = \frac{E_v}{X} A_e = \frac{E_v}{X}$) and subsequently, the dimensionless damage parameter $S = \frac{A_e}{D_n^2}$.

Table 2 summarizes the thresholds of S, for different damage levels, according to [12] and the Rock Manual (2007).

The equipment used for damage evolution assessment was the Microsoft Kinect© position sensor that was placed above the breakwater, to get a 3D model of the armour layer.

The acquisition of depth values by the Kinect© is determined by the Time of Flight (ToF) method, where the distance between the points of a surface and the sensor is measured by the time of flight of the light signal reflected by the surface. In other words, ToF imaging refers to the process of measuring the depth of a scene by quantifying the changes that an emitted light signal encounters when it bounces back from objects in a scene.

The Kinect sensor was positioned 1.5 m from the crest of the structure in a fixed structure above the flume (Fig. 5a) and its survey parameters were: Voxel (volume pixel) for meter: 256; Voxel volume resolution for the three coordinated axis x, y and z: 512 voxel. That means that the volume of each scanned scene is 2 m x 2 m x 2 m. The acquisition distance range was between 0.5 m and 8 m.

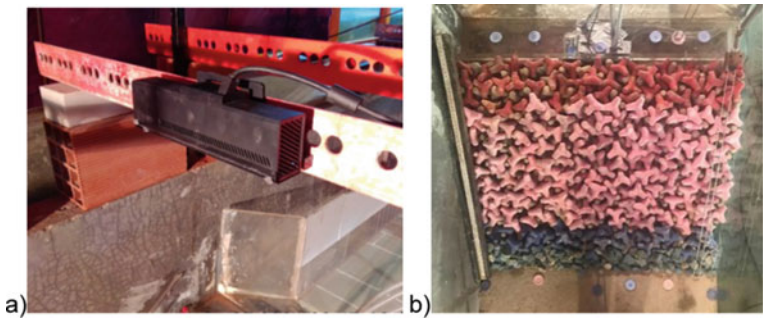

Fig. 5 **a** Position sensor Kinect. **b** Ground control points

Note that the voxel is a 3D unit of the image, just as for digital photographs, a pixel is a 2D unit of the image. It is a volume element that represents a specific grid value in 3D space.

Surveys were carried out without water in the flume, at the beginning and at the end of each test series, and with water at the end of each intermediate test.

To reference the point clouds resulting from the surveys, 12 ground control points (GCP) were used, Fig. 5b. They were materialized with coloured buttons placed at the bottom of the channel, in front of the toe of the armour layer and on the superstructure. The coordinates of these control points were obtained with a total station before the start of the test series.

The post-processing of surveys conducted with water in the flume, comprised a previous alignment of the point clouds with a cloud obtained without water in the flume, to correct the submerged part of the survey, as the infrared light from the sensor has little capacity to cross water depths greater than 0.05 m. This fine alignment was performed using the Iterative Closest Point, ICP algorithm [13] available in the open-source software CloudCompare [14].

The eroded volume computation relied on the gridding process of the cloud(s), by choosing a grid step. This step defines the size of the elementary cells used in the volume computation. To compute the volume, *CloudCompare* sums the contribution of each cell. This contribution is the volume of the elementary parallelepiped corresponding to the elementary cell area, multiplied by the distance difference between clouds ($dV = grid\ step * grid\ step * distance$).

In the present work, after several experiences with grid steps ranging from 1 to 10 mm, the best combination of point density and depth estimation was obtained with a step of 2 mm. Steps smaller than 2 mm conducted to an overestimated depth, while grid steps higher than 2 mm led to an important loss of point density.

4 Results and Discussion

From the damage characterization resulting from the survey of the armour layer of the entire breakwater usable section, it was possible to compute the overall eroded volume. Thus, an averaged eroded area was computed by dividing the eroded volume by the section width (0.72 m). Note that, as the eroded area is an average value, eroded areas in different individual profiles can differ from this value, depending on the heterogeneity of the damage location. Figure 6 shows the point cloud resulting from surveys carried out with the Kinect© sensor at the beginning and at the end of series A (before Test 59 and after Test 81, respectively), as well as the map of distances between both point clouds.

The results presented in Table 3 show the damage values (S) measured at the end of each test run, with a duration of 1000 waves, corresponding to a given wave condition tests 1 to 6, for test series A. According to Table 2, the damage level is clearly at "start of damage" with small variations with the water level and with the peak period, increasing with the significant wave height (Fig. 7).

For test series B (Fig. 8 and Table 4) the damage evolution trend was quite different from the long-duration test A. Damage increases with the water level and with the peak period. At the end of the LWL tests, the damage level denotes a start of damage but at the beginning of tests with HWL the damage level rose to "Intermediate Damage" (Fig. 9).

For test series C (Fig. 10 and Table 5) there is a "start of damage" level, showing no evolution during the test series. Damage stabilization occurred at the end of the tests with HWL, with almost no variation during tests conducted with LWL and Tp = 1.70 s (Fig. 11).

For test series C there is a "start of damage" level, showing no evolution during the test series. Damage stabilization occurred at the end of test with HWL, with almost no variation during tests conducted with LWL and Tp = 1.70 s (Fig. 10).

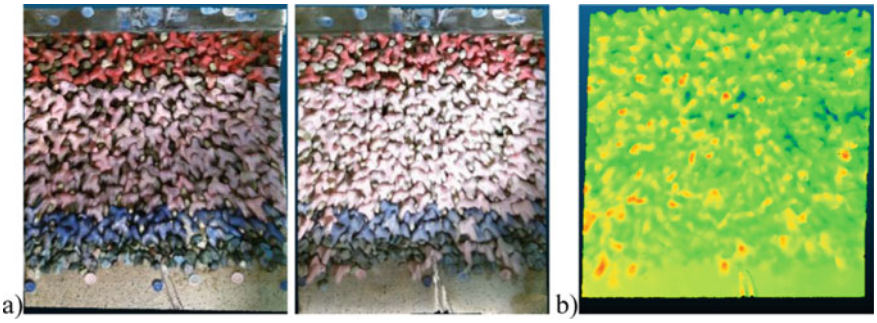

Fig. 6 Survey conducted at the beginning and at the end of test series A. **a** Clouds of points of initial and final surveys. **b** Distance map (blue: erosion; red: deposition)

Table 3 Dimensionless damage parameter obtained during test Series A

Test	Test run	Number of waves	S (Ae/Dn^2)
1	59	1000	1.40
	60	2000	1.40
	61	3000	1.50
2	62	4000	1.30
	63	5000	1.40
	64	6000	1.60
	65	7000	1.30
3	66	8000	1.30
	67	9000	1.40
	68	10,000	1.30
	69	11,000	1.30
4	70	12,000	1.40
	71	13,000	1.40
	72	14,000	1.40
	73	15,000	1.70
5	74	16,000	1.40
	75	17,000	1.40
	76	18,000	1.50
	77	19,000	1.50
6	78	20,000	1.40
	79	21,000	1.60
	80	22,000	1.90
	81	23,000	1.90

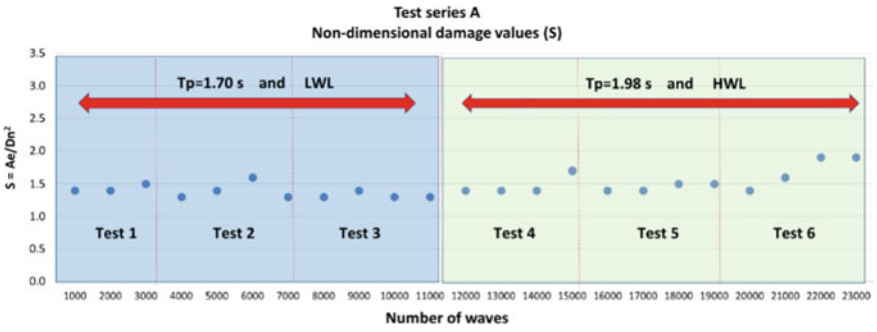

Fig. 7 Damage evolution during test series A

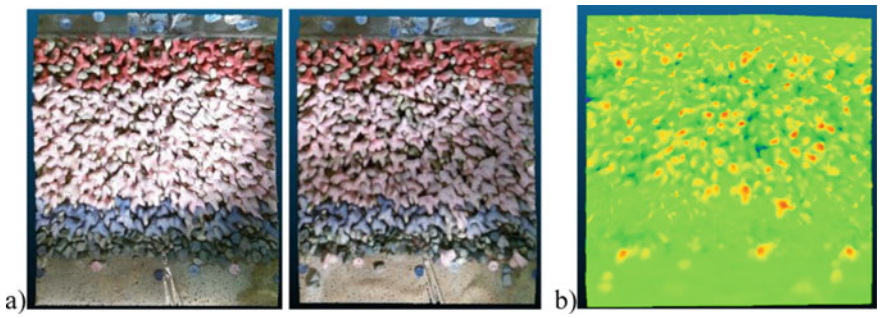

Fig. 8 Survey conducted at the beginning and at the end of test series B. **a** Clouds of points of initial and final surveys. **b** Distance map (blue: erosion; red: deposition)

Table 4 Dimensionless damage parameter obtained during test series B

Test	Test run	Number of waves	S (Ae/Dn^2)
1	82	1000	1.60
2	83	2000	1.20
	84	3000	1.40
	85	4000	1.40
	86	5000	1.20
3	87	6000	1.20
	88	7000	1.50
	89	8000	1.80
	90	9000	1.70
5	91	10,000	2.30
	92	11,000	2.90
	93	12,000	3.00
	94	13,000	2.80
6	95	14,000	3.00
	96	15,000	2.80
	97	16,000	2.90
	98	17,000	2.20

5 Conclusions

This paper described the three scale model test series (A, B and C) with different test sequences and durations, whose objective was to evaluate damage evolution of a stretch of the Peniche harbour west breakwater.

Damage measurement was made using the Kinect© position sensor, which proved to be quite effective in obtaining three-dimensional surface models of the armour

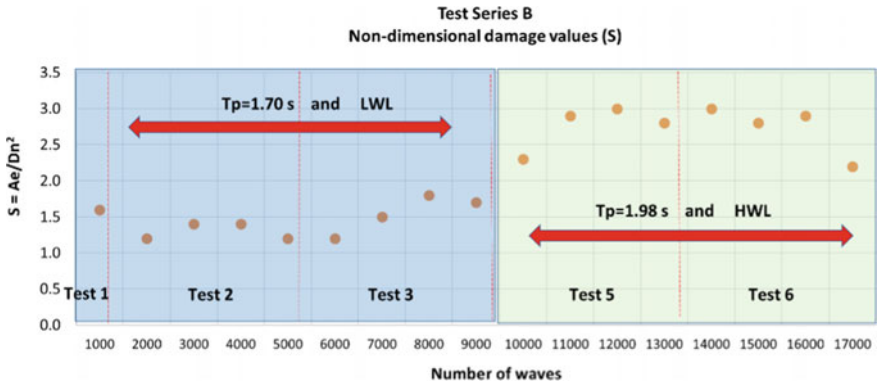

Fig. 9 Damage evolution during test series B

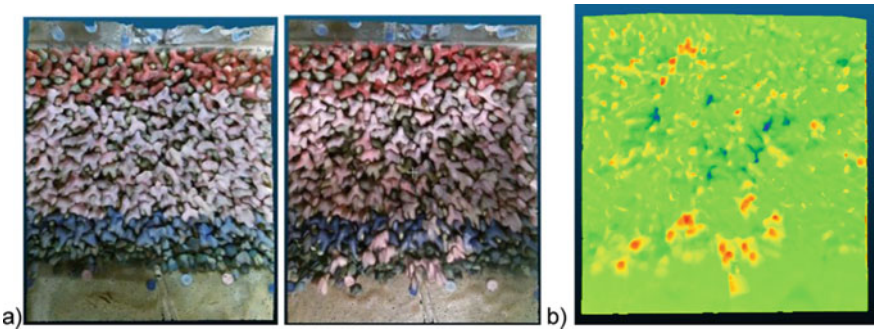

Fig. 10 Survey conducted at the beginning and at the end of test series C. **a** Clouds of points of initial and final surveys. **b** Distance map (blue: erosion; red: deposition)

layers (tetrapods) of the breakwater model. It was possible to obtain damage measurements, such as volume and eroded area. The comparison between initial and final clouds of points resulting from the model survey, enabled to compute the eroded volumes.

The damage descriptor S computation was based upon the eroded volume and evolved with different trends for the three-test series.

For the longest test series, series A, which aims to confirm the stabilization of damage of the armour layer when subjected to a sea state with constant characteristics, the damage level is a "start of damage" with small variations with the water level and with the peak period, increasing with the significant wave height.

Regarding test series B conducted with increasing water levels ant peak periods, damage increases with the water level and with the peak period.

Results obtained with test series C, with decreasing water levels and peak periods, showed no evolution during the test series. Damage stabilization occurred at the end of test with HWL (start of damage), with almost no variation during tests conducted with LWL and Tp = 1.70 s.

Table 5 Dimensionless damage parameter obtained during test series C

Test	Test run	Number of waves	S (Ae/Dn^2)
4	99	0	2.00
	100	1000	2.00
5	101	2000	2.00
	102	3000	2.10
	103	4000	2.00
	104	5000	1.90
6	105	6000	2.10
	106	7000	2.00
	107	8000	2.10
	108	9000	2.00
2	109	10,000	1.90
	110	11,000	1.90
	111	12,000	1.90
	112	13,000	1.90
3	113	14,000	1.90
	114	15,000	1.90
	115	16,000	2.00
	116	17,000	1.90

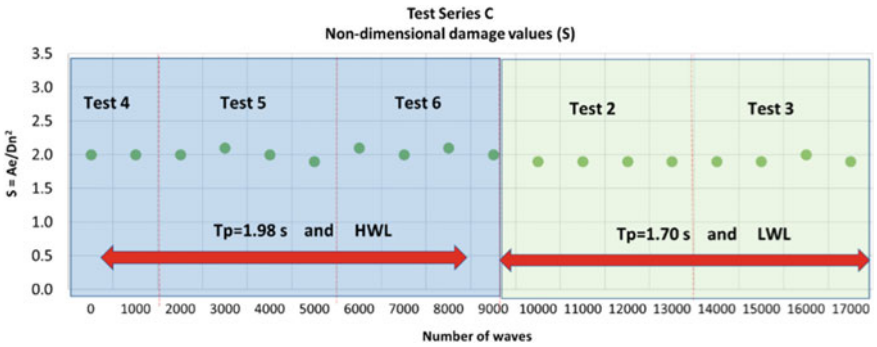

Fig. 11 Damage evolution during test series C

Test series B and C, with the same wave conditions, but with different sequences, conducted to a different damage evolution. Despite both tests conducted to a mild damage, series B proved to be the most unfavourable test sequence.

Future work will comprise tests with localized damage, with more extensive damage levels, to test a dimensionless damage parameter based upon localized eroded volume, as well as on the dimensionless eroded depth.

Acknowledgements This work was carried out within the scope of the projects: PTDC/ECI-EGC/31090/2017 BSafe4Sea and PTDC/EAM-OCE/31207/2017 To-Sealert, both funded by the Portuguese Research Foundation (FCT).

References

1. van der Meer, J.W.: Rock slopes and gravel beaches under wave attack. Ph.D. Thesis, Delft Hydraulics communication no. 396, Delft Hydraulics Laboratory, Delft, The Netherlands (1988)
2. Hofland, B., Disco, M.A.R.K., Van Gent, M.R.A.: Damage characterization of rubble mound roundheads. In: Proceedings of CoastLab2014, Varna, Bulgaria (2014)
3. Hofland, B., et al.: Measuring damage in physical model tests of rubble mounds. In: Coasts, Marine Structures and Breakwaters 2017: Realising the Potential, pp. 929–940. ICE Publishing (2018)
4. Campos, A., Castillo, C., Molina-Sanchez, R.: Damage in rubble mound breakwaters. Part II: review of the definition, parametrization and measurement of damage. J. Mar. Sci. Eng. **8**(5), 306 (2020)
5. Ferreira, R., Costeira, J.P., Santos J.A.: Stereo reconstruction of a submerged scene. In: Marques, J.S., Pérez de la Blanca, N., Pina, P. (Eds.) Pattern Recognition and Image Analysis. IbPRIA 2005. Lecture Notes in Computer Science, vol. 3522. Springer, Berlin, Heidelberg (2005)
6. Lemos, R., Santos, J.A., Fortes, C.J.: Rubble mound breakwater damage assessment through stereo photogrammetry in physical scale laboratory tests. Ribagua **4**(2), 84–98 (2017)
7. Musumeci, R.E., et al.: 3-D monitoring of rubble mound breakwater damages. Measurement **117**, 347–364 (2018)
8. Sande, J., et al.: Application of scanning techniques for damage analysis in rubble mound breakwaters. In: Proceedings of 7th International Conference on the Application of Physical Modelling in Coastal and Port Engineering and Science (Coastlab18), Santander (2018)
9. Campos, A., Castillo, C., Molina-Sanchez, R.: Damage in rubble mound breakwaters. Part I: historical review of damage models. J. Mar. Sci. Eng. **8**(5), 317 (2020)
10. Construction Industry Research and Information Association. The Rock Manual. The Use of Rock in Hydraulic Engineering, 2nd edn. CIRIA, London, UK (2007)
11. Broderick, L.: Riprap stability, a progress report. In: Coastal Structures, pp. 320–330. ASCE, Reston, VA, USA (1983)
12. Vidal, C., Losada, M.A., Medina, R., Losada, I.: Análisis de La Estabilidad de Diques Rompeolas. Diques Rompeolas **1**, 17–34 (1994)
13. Chen, Y., Medioni, G.: Object modelling by registration of multiple range images. Image Vis. Comput. **10**(3), 145–155 (1992)
14. Girardeau-Montaut, D.: Détection de changement sur des données géométriques tridimensionnelles. Diss. Télécom ParisTech (2006)